

Recommendations to PA on
Salado Formation Intrinsic Permeability and Pore Pressure
for
40 CFR 191 Subpart B Calculations

June 15, 1992

Elaine Gorham
Richard Beauheim
Peter Davies
Susan Howarth
Stephen Webb

Department 6119

Introduction

In March 1992, the Fluid Flow and Transport Department was asked to recommend Salado Formation permeability and pore pressure probability distributions to be used in the 1992 RCRA calculations for the WIPP. The recommendations were requested and transmitted informally. Eventually a description of the rationale for the recommendations was written by the Fluid Flow and Transport Department and published in Appendix A of (WIPP Performance Assessment Division, 1992A).

Following the RCRA calculations, the Fluid Flow and Transport Department was asked to recommend Salado Formation permeability and pore pressure to be used in the 1992 40 CFR 191 Subpart B compliance calculations. The recommendations transmitted to the PA group in the attached memo by P. D. Davies et al. were based on the, earlier, RCRA recommendations.* The present description is a detailed record of the rationale for the 1992 40 CFR 191 permeability and pore pressure recommendations transmitted in the Davies et al. memo and includes some comments on the adequacy of the current PA models to accurately describe all phenomena present in the formation.

Since input parameters, such as permeability or formation pore pressure, are, for the most part, inferred from complex hydrologic tests, the interpretive model assumptions should be compatible with the predictive or performance assessment model in which the parameters will be used. Thus a suggested excavation geometry and zoning scheme was supplied along with recommended distributions for permeability and pore pressure. The recommended initial geometry is shown in Figure 1 and the distributions suggested for permeability and pore pressure (Table 1 and Figures 2-6) were referenced with respect to those zones.

* Note: The referenced memo is included in this appendix as Davies et al., July 22, 1992.

Our Assumptions

Assumptions about the models to be used in the PA calculations that were essential in formulating the 40 CFR 191 data recommendations were not included in the informal material. Our assumptions were

1. The Salado Formation was described as consisting of layers of either halite or anhydrite. Parts of the Salado Formation described as argillaceous halite were lumped with the halite; clay seams were lumped with the type of lithology in which they occurred. Anhydrites a and b were lumped together.
2. The Salado Formation is isotropic and homogeneous within each layer of halite or anhydrite. The halite and anhydrite have interconnected porosity in pressure equilibrium in the far field. Thus there can be no pre-existing hydraulic pressure differential between stratigraphic layers in the far field Salado Formation.
3. The repository will have been at atmospheric pressure for at least 20 years before final closure. PA will simulate the depressurization in the formation surrounding the repository in a start-up phase which allows brine to flow into a closed repository initially at atmospheric pressure. At the end of the start-up phase, a DRZ will be created; the repository and DRZ pressure will be re-set to atmospheric pressure; the DRZ porosity will be set to a value sampled from a probability distribution; and the brine saturation in the DRZ will be set to preserve the total volume of brine in the DRZ region at the end of the start-up calculation.
4. Excavation closure effects are **not** to be included in the PA model nor is pressurized fracture opening in the anhydrite beds. Pressurized fracture opening in the anhydrite beds may have the potential to significantly increase far-field interbed permeabilities. We were specifically requested by the PA group to **not** include the potential effects of pressurized fracture opening in our recommended permeability distribution for the anhydrite layers, as we suggested in the attached memo from E. Gorham. **Thus we believe the 1992 40 CFR 191 compliance calculations may underestimate lateral gas migration in the interbeds and overestimate repository pressurization.**
5. The nature of the disturbed rock zone (DRZ) is uncertain, reflecting the diversity of technical hypotheses that have been formulated, documented and undocumented. These include the hypothesis that the DRZ is a zone of increased porosity surrounding the excavation, that is stable in extent or increasing in extent with the age of the excavation. Other hypotheses concerning the nature of the DRZ are that the bulk properties of the halite within the DRZ are unchanged, but that within the DRZ fractures form that result in a large increase in permeability with a relatively small increase in porosity or storativity within the DRZ. The size of the DRZ can vary from a few inches into the formation from an excavation surface to a few "room-radii" away from the excavation

surface. It was assumed that all possible descriptions of the DRZ should be included in the probability distributions for permeability and porosity in the DRZ.

6. The DRZ does not reconsolidate during the post-closure calculations due to repository re-pressurization or creep closure of the excavation.

Sources of uncertainty in interpreting data.

The process of inferring permeability from a hydrologic pulse or shut-in test requires that one make an assumption about the diffusivity or specific storage in the formation, about the size of a damaged zone surrounding the test zone, and that the compressibility of the test-zone fluid is constant and can be quantified by a single measurement of fluid withdrawn from the test zone vs test zone pressure drop during withdrawal. A value of specific storage calculated using literature values for halite and brine compressibilities may not be correct. Recent improvements in the measurement of permeability involve combining a constant-pressure flow test and a shut-in test to directly infer a value of specific storage. However, the improved interpretive technique was used only on permeability tests SCP01, S1P73-B, C1X10, L4P52-A and L4P51-B. For the remaining permeability tests, what is in reality obtained is a value of permeability **given an assumed value of specific storage**. Sensitivity calculations have shown that our inferred permeability values may range over one order of magnitude as our assumed values of specific storage range over three orders of magnitude. (Beauheim et al, 1990; Beauheim et al, 1992) Inasmuch as our assumed values of specific storage do not range over more than three orders of magnitude, we estimate our uncertainty in permeability to be about an order of magnitude.

Other assumptions in analysis of permeability tests include the assumption that gas dissolved in formation brine does not significantly affect the permeability interpretation and that significant amounts of free gas are not present in the formation. In numerous permeability tests, gas was observed to bubble from the formation shortly after the test zone was drilled. A sensitivity analysis is planned for FY93 in which the effect of these phenomena on permeability interpretation will be investigated. For the RCRA recommendations, Rick Beauheim, who has been conducting interpretations of permeability tests, provided the (subjective) input that resulted in an order of magnitude confidence in interpreted permeability values.

Uncertainties in the interpretation of brine-inflow tests are due to (a) scatter in the brine-inflow data and (b) the use of a one-dimensional model which neglects loss of fluid to the surface of the excavation and assumes a uniform pore pressure unaffected by the excavation. In a one-dimensional data analysis by McTigue (1992), it was found that the uncertainties in the inferred values of diffusivity due to data scatter could be substantial.

Uncertainties in inferred values of permeability may be smaller. (See Table 2.) In addition, recent analyses (Gelbard, 1992) indicate that the use of a one-dimensional model may introduce significant errors in the interpretation of diffusivity and permeability from brine-inflow data.

Rationale for Formulating Permeability Distributions

Table 3 represents a current (as of 1/5/92) compilation of interpreted values of permeability and formation pressure from the Permeability Testing Program, the Small-Scale Brine Inflow Program and Room Q. For the 1992 40 CFR 191 Subpart B calculations, interpreted values of permeability in Table 3 were classified according to the regional map shown in Figure 1.

The disturbed rock zone is poorly defined. For these recommendations, test zones were classified as being in the disturbed rock zone if the zone could sustain little or no formation pressure and if the permeability of the zone was clearly higher than expected in competent rock.

The tests for which a reasonable pressure could be sustained in the test zone, but the pressure was not high enough to approach our (subjective) estimate of the far field pressure, were classified as being in a "depressurized" zone. The "depressurized zone" is hypothesized as having experienced some hydraulic depressurization and possibly some elastic stress relief due to the excavation, but probably no irreversible rock damage and large permeability changes. The extent of the depressurized zone may be different in higher permeability layers, such as the Marker Beds, than in lower permeability layers, such as pure halite. It is important to note that the depressurized zone is not a disturbed rock zone; the data from the depressurized zones do not support the hypothesis that the permeability, and the interconnected porosity, are greatly different in the depressurized zones from their far field values.

The latter classifications of test zones are subjective and will be examined in more detail as the Fluid Flow and Transport Department improves interpretation techniques and understanding of the rock matrix.

For the tests in Table 3, other than the Room Q tests, the disturbed rock zone, if in fact it has a clear boundary and if it has a significant extent, was hypothesized to extend about one meter from the excavation into the formation. The boundary of the depressurized zone in the Marker Beds was hypothesized to be approximately 10 meters from the excavation. These hypotheses formed the basis for the geometrical treatment of the excavation suggested in Figure 1. Detailed repository depressurization calculations are planned for FY93.

The PA calculations did not follow the zoning scheme recommended in Figure 1. Only a disturbed rock zone was distinguished from the

far field. Thus it was recommended that the depressurized zone and far field zone tests be combined to form a single permeability distribution.

The probability distributions recommended for the PA calculations were formulated so as to reflect the true range of scientific uncertainty in the parameter values supplied, including uncertainty due to measurement error and uncertainty due to interpretation ambiguities. As mentioned above, an order of magnitude uncertainty in the interpreted value of permeability was used as a rule of thumb for creating recommended probability distributions.

All measurements of permeability were given equal weight, except those values derived from brine inflow measurements in 36" diameter holes in Room D. Those tests were considered flawed and deleted from the list because of the uncertain history of the excavation surrounding the test zone (Finley, 1992).

The hypothesis that permeabilities in the Salado Formation are heterogeneous is given much weight in the Fluid Flow and Transport Department. The use of a single uniform value for all halite and argillaceous halite regions, and a different uniform value for all marker beds implies that the permeability values used in the PA calculations should be "effective" values that are rigorously derived from our measurements. A systematic approach for defining such an "effective" value has not yet been outlined, but will be investigated in FY93. For the 1992 40 CFR 191, Subpart B calculations the values of permeability that were classified as "too low to measure" were represented by effective permeabilities in the range of 10^{-24} to 10^{-22} m², since it was judged that even if the halite contained regions of zero permeability, the likelihood was low that the effective permeability of the halite and argillaceous halite regions was zero.

Given the assumptions, difficulties and exceptions outlined above, differential probability distributions were formed by marking the locations along a permeability axis of the results of the tests in Table 3. Excluding the "too low to measure" permeability tests, the number of tests in each log₁₀ interval were used to indicate the relative probability that the true value lay in that interval. Cumulative probability distributions listed in Table 1 can be formulated from the differential probability distributions in Figures 2-6. Test results that were "Too low to measure" are shown in Figure 2 as lying between a true 0 value and 1.0×10^{-24} m². Thus, the abscissa of Figure 2 is logarithmic between 10^{-24} and 10^{-21} and linear between 0 and 10^{-24} .

Rationale for Formulating Pore Pressure Distributions

The measurement of test-zone pore pressure is straightforward and is only accomplished in the Permeability Testing Program and the Room Q permeability tests. If, during a pressure build-up test or pulse-withdrawal test, the pressure reaches a steady state

pressure, that pressure is interpreted as the formation pore pressure at the location of the test zone. If a steady-state pressure is not reached before the test is terminated, some technique must be used to extrapolate the formation pore pressure from the shape of the pressure-vs-time curve.

For the tests listed in Table 3, all pressures shown are measured or estimated values of formation pore pressure. The far field formation pore pressures measured in the anhydrite layers yield a fairly consistent measurement of 12.5 ± 0.1 MPa. It is not understood why the pore pressure measured in the single halite far field test is significantly lower than those reached in the anhydrite far field. Possibilities include: (a) The regions in the halite that have non-zero permeability are not interconnected with higher pressure regions such as the anhydrite layers; (b) the regions in the halite that have non-zero permeability have not reached pressure equilibrium with the anhydrite layers; or (c) pore dilation (and accompanying depressurization) in response to excavation and/or drilling affects halite to a greater distance than anhydrite.

Based on current measurements, it cannot be ruled out that substantial regions of the Salado Formation will be at significantly lower initial pore pressure than the anhydrite layers. Because of potential computational difficulties the PA group did not wish to include this possibility in the 40 CFR 191 calculations. Use of a uniform hydraulic pressure throughout the formation far field allows the PA calculations to be based on the appealingly simple (although perhaps not correct) assumption of homogeneity, hydraulic equilibrium and isotropy in the undisturbed Salado Formation. (The assumption of formation hydraulic equilibrium can be tested using existing models and assumed values of halite and anhydrite permeability. Such a calculation may be performed by Department 6119 in the future.)

Since the effect of excavation on the formation is still poorly understood, from a hydrological viewpoint, it is uncertain that tests believed to be in the far field are indeed in the far field. It was recommended that the far field pore pressure reflect the average of the three far field measurements in the anhydrite, 12.5 MPa, with an uncertainty of 0.5 MPa.

Comments on the Effect of Data Recommendations on 40 CFR 191 Subpart B Compliance Calculations.

An important aspect of the current PA model for the Salado Formation is its inability to simulate pressure-induced fracturing in the anhydrite layers, a phenomenon that has been experimentally demonstrated at the WIPP. The phenomenon may enhance the migration of gas into the formation as the gas pressure in the repository builds up.

Thus it should be recognized that the data from which the permeability and pore pressure recommendations have been derived may not fully support the existing performance assessment models. While it might have been possible to adjust the input parameter distributions to crudely include effects not explicitly modeled, such as including post-fracture permeability in the far field anhydrite permeability distribution to include the phenomena of pressure-induced fracturing, this approach was unacceptable to the performance assessment group. Therefore, it is important to understand that the 1992 performance assessment calculations will not reflect the full range of potential outcomes. In other words, the calculations do not include all known or possible phenomena and outcomes.

References:

Beauheim, R. L., G. J. Saulnier, Jr. and John D. Avis. 1990. **Interpretation of Brine-Permeability Tests of the Salado Formation at the Waste Isolation Pilot Plant Site: First Interim Report.** SAND90-0083. Albuquerque, NM: Sandia National Laboratories.

Beauheim, R. L., T. F. Dale, M. D. Fort, R. M. Roberts and W. A. Stensrud. 1992. **Hydraulic Testing of Salado Formation Evaporites at the Waste Isolation Pilot Plant Site: Second Interpretive Report.** SAND92-0533. Albuquerque, NM: Sandia National Laboratories.

Gelbard, F. 1992. **A Two-Dimensional Model for Brine Flow to a Borehole in a Disturbed Rock Zone.** SAND92-1303. Albuquerque, NM: Sandia National Laboratories.

McTigue, D. F. 1992. **Permeability and Hydraulic Diffusivity of WIPP Repository Salt Inferred from Small-Scale Brine Inflow Experiments.** SAND92-1911. Albuquerque, NM: Sandia National Laboratories.

WIPP Performance Assessment Division. 1992A. **Preliminary Comparison with 40 CFR Part 191, Subpart B for the Waste Isolation Pilot Plant, December 1991.** SAND91-0893/6. Albuquerque, NM: Sandia National Laboratories.

Table 1. Recommended Cumulative Probability Distributions for formation permeability (m^2), derived from Figures 2-6.

Halite Far Field and Depressurized Zones: Zones A, B and C

Permeability (m^2)	Cumulative probability
0.0	0.00
1.0×10^{-24}	0.00
1.0×10^{-23}	0.10
1.0×10^{-22}	0.19
1.0×10^{-21}	0.48
1.0×10^{-20}	0.95
1.0×10^{-19}	1.00

Halite Disturbed Zone: Zones D and E

Permeability (m^2)	Cumulative probability
1.0×10^{-18}	0.00
1.0×10^{-13}	1.00

Table 1. (Continued)

Anhydrite Far Field and Depressurized Zones: Zone F, G and H

Permeability (m²) Cumulative probability

1.0x10 ⁻²¹	0.00
1.0x10 ⁻²⁰	0.07
1.0x10 ⁻¹⁹	0.71
1.0x10 ⁻¹⁸	0.93
1.0x10 ⁻¹⁷	0.96
1.0x10 ⁻¹⁶	1.00

Anhydrite Disturbed Zone: Zone J

Permeability (m²) Cumulative probability

1.0x10 ⁻¹⁸	0.00
1.0x10 ⁻¹⁷	0.12
1.0x10 ⁻¹⁶	0.25
1.0x10 ⁻¹⁵	0.37
1.0x10 ⁻¹⁴	0.75
1.0x10 ⁻¹³	0.87
1.0x10 ⁻¹²	1.00

Anhydrite Disturbed Zone: Zone I

Permeability (m²) Cumulative probability

1.0x10 ⁻¹⁹	0.00
1.0x10 ⁻¹⁸	1.00

Table 2. Parameter Estimates from Borehole Experiments. This from information in Table 5 of an early draft of McTigue, 1992. The difference between the values from the early draft (this table) and the table in McTigue, 1992 is the use of a literature value and a WIPP-specific measured value, respectively, for brine compressibility in the data interpretation.

Borehole #	Rock Type	Permeability @Po=10 MPa (m ²)	Permeability @Po=5 MPa (m ²)	Permeability @Po=01MPa (m ²)	Diffusivity (m ² /sec)
DBT10	Halite	2.9E-22±.18E-22	5.8E-22±.36E-22	2.9E-21±.18E-21	4.7E-11±.78E-11
DBT11	Halite	1.1E-21±.09E-21	2.3E-21±.18E-21	1.1E-20±.09E-20	3.5E-9±.63E-9
DBT12	Halite	6.4E-22±.72E-22	1.3E-21±.14E-21	6.4E-21±.72E-21	10E-8±.65E-8
DBT13	Halite	1.7E-22±.26E-22	3.4E-22±.32E-22	1.7E-21±.26E-21	5.9E-11±.2.3E-11
DBT14A	Halite	7.8E-22±.2.4E-22	1.6E-21±.48E-21	7.8E-21±.2.4E-21	2.8E-8±4.6E-8
DBT14B	Halite	2.2E-21±.28E-21	4.5E-21±.56E-21	2.2E-21±.28E-21	4.3E-8±3.3E-8
DBT15A	Halite	3.2E-22±.55E-22	6.4E-22±1.1E-22	3.2E-21±.55E-21	1.8E-10±.86E-10
DBT15B	Halite	1.8E-22±.59E-22	3.6E-22±1.1E-22	1.8E-21±.59E-21	1.3E-10±1.2E-10
L4B01	Halite	.67E-22±.43E-22	1.3E-22±.86E-22	.67E-21±.43E-21	5.8E-11±9.1E-11
DBT31A	Halite	9.0E-22±2.4E-22	1.8E-21±.48E-21	9.0E-21±.2.4E-21	1.27E-10±.22E-11
QPB01 *1	Anhydrite	4.8E-21±.3E-21	9.6E-21±.06E-21	4.8E-20±.3E-20	1.1E-8±.34E-8
QPB02 *1	Anhydrite	8.2E-20±.03E-20	1.6E-19±.006E-19	8.2E-19±.03E-19	1.2E-9±.014E-9
QPB03 *1	Anhydrite	4.8E-21±1.5E-21	9.6E-21±.3E-21	4.8E-20±1.5E-20	6.4E-7±18.8E-7*

* The lower limit of these uncertainty bounds should be assumed to be zero.

*1 For all of these borehole tests, the length of the productive unit was assumed to be equal to the average thickness of Marker Bed 139 (3-fect).

Table 3: Compilation of Interpreted Values of Permeability, 1/5/92. Zones are referenced to Figure 1.

<u>Zone</u>	<u>Test</u>	<u>Measured Permeability</u>	<u>Pressure(MPA)</u>
A. HALITE FAR FIELD			
	QPP12 pre-mineby		
		$6.8 \times 10^{-22} \text{ m}^2$	9.5
	C2H03	Too low to measure	not measureable
	SCP01 GZ	Too low to measure	not measureable
	QPP05	Too low to measure	not measureable
	QPP02	Too low to measure	not measureable

B. HALITE DEPRESSURIZED ZONE

S1P72-A-GZ	$8.6 \times 10^{-22} \text{ m}^2$	5.1
QPP21 post mineby		
	$1.9 \times 10^{-22} \text{ m}^2$	4.8
C2H01-B	$5.3 \times 10^{-21} \text{ m}^2$	3.1
C2H01-B-GZ	$1.9 \times 10^{-21} \text{ m}^2$	4.1
L4P51-A	$6.1 \times 10^{-21} \text{ m}^2$	2.7
S0P01	$8.3 \times 10^{-21} \text{ m}^2$	4.4
S1P71-A	$6.1 \times 10^{-20} \text{ m}^2$	2.9
QPP15	$2.2 \times 10^{-21} \text{ m}^2$	3.1
DBT10	$5.8 \times 10^{-22} \text{ m}^2$	5.0 assumed
DBT11	$2.3 \times 10^{-21} \text{ m}^2$	5.0 assumed
DBT12	$1.3 \times 10^{-21} \text{ m}^2$	5.0 assumed
DBT13	$3.4 \times 10^{-22} \text{ m}^2$	5.0 assumed
DBT14A/B	$3.1 \times 10^{-21} \text{ m}^2$	5.0 assumed
DBT15A/B	$5.0 \times 10^{-22} \text{ m}^2$	5.0 assumed
L4B01	$1.3 \times 10^{-22} \text{ m}^2$	5.0 assumed
DBT31A	not used	
QPP12	$4.4 \times 10^{-22} \text{ m}^2$	9.4

C. HALITE DEPRESSURED ZONE

Same as region B for permeability.

D. HALITE DISTURBED ROCK ZONE

C2H01-A	$2.7 \times 10^{-18} \text{ m}^2$	0.5
C2H01-A-GZ	unmeasureable	0.0
S1P73-B-GZ	unmeasureable	2.5

E. HALITE DISTURBED ROCK ZONE

Same as region D for permeability.

Table 3. (Continued)

F. ANHYDRITE FAR FIELD (greater than 10 m from excavation)

SCP01 MB 139	$3.0 \times 10^{-20} \text{ m}^2$	12.4
QPP13 pre-mineby MB 139	$4.1 \times 10^{-20} \text{ m}^2$	12.5
QPP03 pre mineby clay b	$4.4 \times 10^{-20} \text{ m}^2$	12.6

G. ANHYDRITE DEPRESSURIZED ZONE (less than 10 meters from excavation)

C2H02 MB 139	$7.8 \times 10^{-20} \text{ m}^2$	9.3
L4P51-B anhydrite c	$5.0 \times 10^{-20} \text{ m}^2$	5.1
S1P71-B anhydrite c	$6.8 \times 10^{-20} \text{ m}^2$	4.9
C2H01-C MB 139	$9.5 \times 10^{-19} \text{ m}^2$	8.0
C1X10 MB 139	$5.0 \times 10^{-17} \text{ m}^2$	7.3
QPP03 anhydrite b post mineby	$7.9 \times 10^{-20} \text{ m}^2$	7.0
QPP13 MB 139 post mine-by	$4.7 \times 10^{-20} \text{ m}^2$	8.1
L4P52-A anhydrite a	$1.0 \times 10^{-19} \text{ m}^2$	6.4
QPB01	$9.6 \times 10^{-21} \text{ m}^2$	5.0 assumed
QPB02	$1.6 \times 10^{-19} \text{ m}^2$	5.0 assumed
QPB03	$1.2 \times 10^{-20} \text{ m}^2$	5.0 assumed
S1P72	unmeasureable	1.2

H. ANHYDRITE DEPRESSURIZED ZONE
Same permeability as region G.

I. ANHYDRITE DISTURBED ROCK ZONE (138)

S1P73-B MB 138	$2.9 \times 10^{-19} \text{ m}^2$	4.5
----------------	-----------------------------------	-----

J. ANHYDRITE DISTURBED ROCK ZONE

SOP01 GZ	$5.7 \times 10^{-18} \text{ m}^2$	0.5
S1P73-A	too high to measure; estimated at 10^{-15} m^2	0.0
S1P73-A-GZ	too high to measure; estimated at 10^{-15} m^2	0.0
S1P71-A-GZ	too high to measure; estimated at 10^{-14} m^2	0.0
L4P51-A-GZ	too high to measure; estimated at 10^{-15} m^2	0.3
Crawley	$1.6 \text{ to } 3.2 \times 10^{-13} \text{ m}^2$???

YET TO BE INTERPRETED

QPP01
QPP04
QPP11
QPP14
QPP22
QPP23
QPP24
QPP25

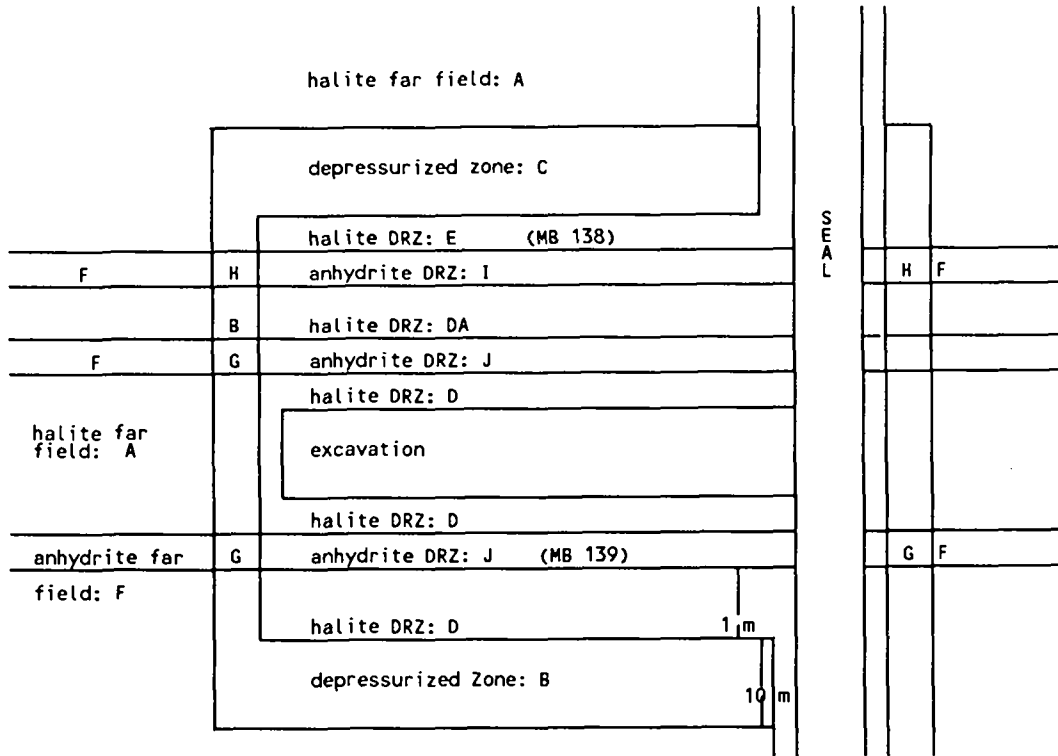


Figure 1: Schematic for assigning flow properties to Salado Formation (Not to Scale!!!!)

Halite Far Field and Halite Depressurized Zone: Zones A, B and C

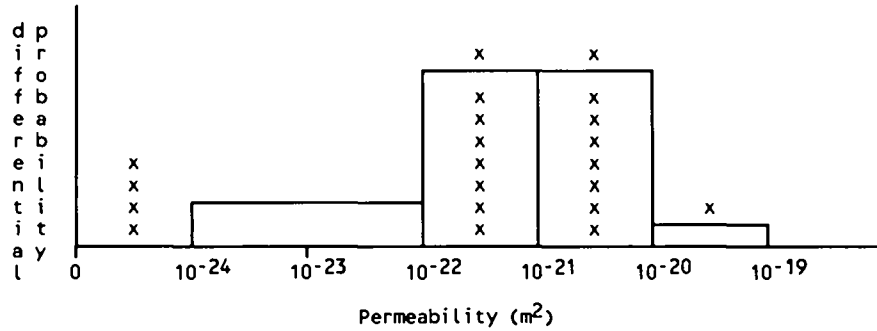


Figure 2.

Halite Disturbed Zone: Zones D and E

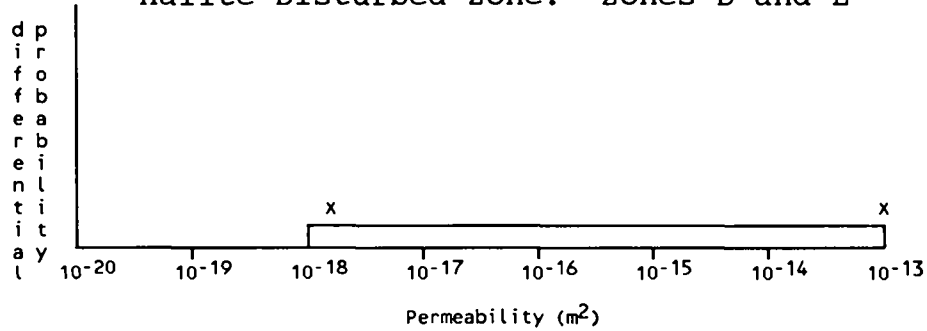


Figure 3.

Anhydrite Far Field and Anhydrite Depressurized Zone: Zones F, G and H

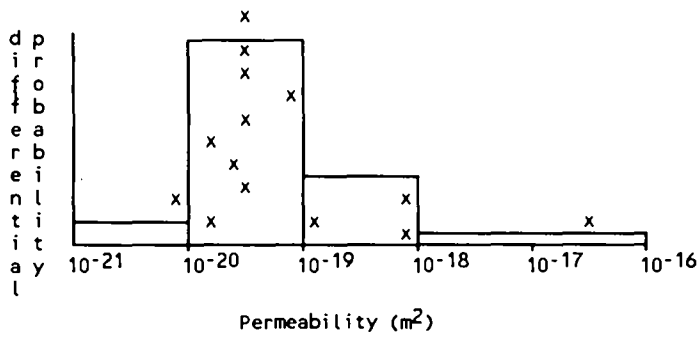


Figure 4.

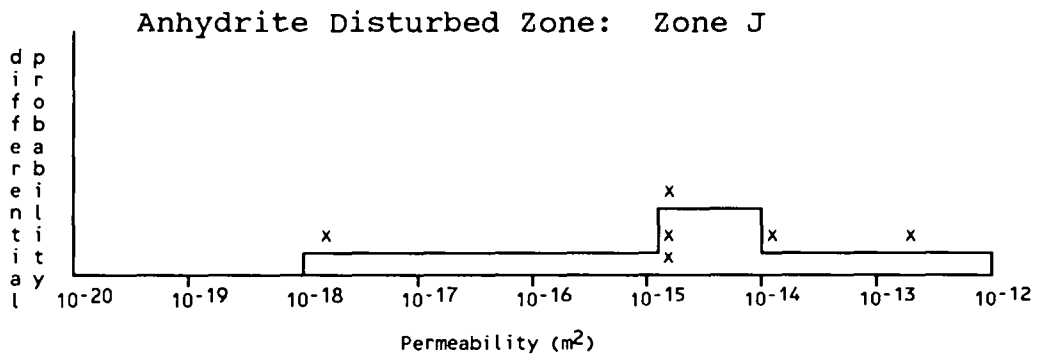


Figure 5.

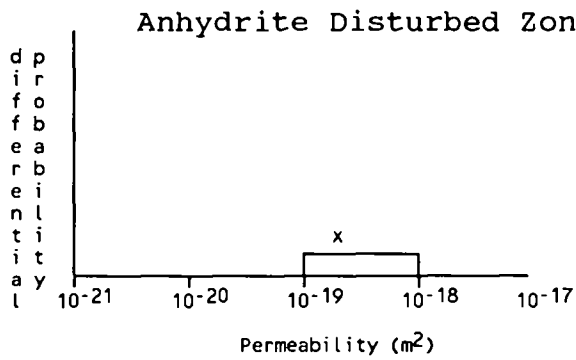


Figure 6.